GLOBAL JOURNAL OF ENGINEERING, DESIGN & TECHNOLOGY
(Published By: Global Institute for Research & Education)
www.gifre.org

STUDY THE EFFECT OF ULTRASONIC TREATMENT ON POROUS SILICON RAMAN PEAK SHIFT

Yasmeen Zaidan Dawood
University of Mustansiriya,
Collage of Education, Department of Physics, Baghdad, Iraq.

Abstract

In this work, an ultrasonically enhanced chemical etching, to fabricated porous silicon layer. Porous silicon layer is fabricated in p-type (111) orientation silicon by using HF solution, and HNO_3. It was found the structure of PS layer on p-type Si was improved by ultrasonic.Ultrasonically enhanced chemical etching is developed to fabricate luminescent porous silicon (PS) material.By applying ultrasonically enhanced etching, PS microcavities with much higher quality factors can be fabricated. The effect is attributable to effective change in the concentration of free holes carriers. Raman scattering measurement on (111) oriented Pp-type crystalline silicon (c-Si) and PS samples were carried out. Raman scattering from the optical phonon in PS showed the red shift of the phonon frequency, broadening and increased asymmetry model of the Raman mode on increasing the power of US. Using the phonon confinement model, the average diameter of Si nanocrystallinies has been estimated a 9nm and 10nm for 30W and 50W.the relationship between the width, shift and asymmetry of the Raman line is calculated and is in a good agreement with available experimental data.

Keywords: Porous silicon, chemical etching, ultrasonic treatment and Raman spectroscopy.

1. Introduction

Since the discovery of its visible photoluminescence and electroluminescence at room temperature, porous siliconPS has been considered a very attractive material for applications in the entirely silicon based optoelectronics [1-5]. PShas an extremely large internal surface area3 resulting in a chemical reactivity of PS to the ambient and in an instability of its properties with time. The study of species inside PS can be useful to solve problems related to the aging and capping of PS, to control impurities and the adsorption on pore walls, to design structures with well defined properties, Raman spectroscopy, including measurements can be an important tool for monitoring all these processes. Unfortunately, the Raman signal of the observed species is usually very weak, hence an improvement of sensitivity would be desirable [6-9].

Since Canham discovered the efficient visible light emission from highly porous silicon (PS),' considerable attention has been paid to investigating its structural and electronic properties. Raman scattering spectroscopy is one of the powerful techniques for studying structure related information, especially information concerning nanostructures in crystalline materials. The study of Raman spectroscopy and photoluminescence (PL) of PS and attributed the Raman peak shift of PS to the effect of phonon confinement, also conducted Raman studies on PS, with emphasis on the line widths and peak shifts of Raman spectra [10-14].

However, the spectra they observed were very broad, with a tail extending to a wave number much lower than 480 cm-'. It is very likely that some contribution from the amorphous phase may be involved in the light scattering. The possible inclusion of any amorphous band would make interpretation of the experimental line shape very difficult. In addition, the effect of the strain that may exist in PS was not considered in any of the previous studies [15-19]. Porous silicon (PS) has stimulated great interest in the photovoltaic community due to its light trapping and antireflection properties [1].In addition, the simultaneous formation of a selective emitter may be achieved by converting into PS the uppermost emitter cell region between the grid contact fingers. PS can be formed by chemical or electrochemical etching of the completed solar cell. Chemical etching(also called stain etching) is more adapted to industrial fabrication due to its simplicity and lower cost [17-20].

The objective of this work is to investigate the effect of ultrasound (US) on the formation of porous semiconductors. The effect of US on semiconductor processing could play an important role in determining the size of micropores in porous semiconductor. The US, on the other hand, can have similar effects such as the changes in density and crystal size through the process of sono cavitation. There have already been successful applications using the US cavitation to the synthesis of materials [20].

Raman spectra of porous silicon have been extensively studied, since the width of the Raman band observed. The optical phonon is sensible to the crystallite size due to the confinement of phonon. It was expected that Raman bands give information on microstructure of material, and therefore, would be suitable in the investigation of the effect the frequency on PS layer formation.

2. Experimental Work

The porous silicon was prepared by chemical etching p-type (111) oriented silicon (sheet resistivity 5.25Ω/□) was used. PS layers were prepared in ($HF:HNO_3:H_2O$) at (1:2:1) respectively.Etching time was 20 min. For the using ultrasonically cavity through the etching processes to enhanced chemical etching (frequency 22 kHz, US power 30W and

50W)..Raman spectra were recorded at room temperature in 45º reflection geometry using 5145Åline of argon ion laser as excitation source which has a penetration depth of about 100nm in c-Si, and computer controlled SPEX Ramalog (model 14018) equipped with a cooled photomultiplier tube and a photon counting system.

3. Results

Figure 1 give a typical Raman spectrum of PS samples that were etched for 20min. The spectrum from a crystalline Si wafer is also shown for comparison. The peak position and width of the sample in Figure 1(a) only have small changes as compared to those of c-Si. The Raman-line peak position shifts to a lower frequency of 521 cm^{-1} after etching, as shown in Figure 1.

Furthermore, the Raman line is wide and asymmetric in comparison to the Raman line from crystalline silicon, for which the line is narrow and symmetric, centered at 520 cm^{-1}.The fit was very good and the peak position *w(q)* and the full width at half maximum (Γ) were obtained as 521 cm^{-1} and 3.5 cm^{-1}, respectively. Crystalline quality of *c*-Si is very good since Γ is close to the instrumental resolution (4.4 cm^{-1}). (Γa and Γb being the half-width on the low and high-energy sides from the center of peak position, respectively). Comparing the Raman spectra from PS with that of c-Si, one can see the Raman line of the PS is red shift and highly asymmetric. It is known that the asymmetric Raman line shape can arise due to the phonon confinement in nanoscale crystallites [6, 15]. But the peak intensity of the PS sample is several times stronger than that of c-Si, which is believed due to the remarkable change of its optical constants. In contrast to the scattering from c-Si, the scattering light from porous silicon is depolarized, indicating a breakdown of the scattering selection rules for the (100) surface.

The average size of nanostructures probed in Raman spectroscopy experiment can be determined by employing the phonon confinement model. This model is based on the fact that optical phonons at the center of the Brillouin zone (q=0) contribute to the first-order Raman model at 521cm^{-1} from c-Si. For nanocrystals, the momentum conversation criterion is relaxed due to a breakdown of full translational symmetry and optical phonons are confined within the nanostructures. This allows optical phonons with (q≠0) to make additional contributions to the first order Raman scattering. Therefore, the first order Raman intensity I′(w, L) for spherical nanocrystallite with three dimensional confinement can be written as [10, 14, 20]:

$$I'(w) = \int_0^1 \frac{|C(q)|^2}{\left\{[w - w(q)]^2 + (\frac{\Gamma}{2})^2\right\}} dq \quad (1)$$

$$|C(q)|^2 = \exp\left(-\frac{q^2 L^2}{4a^2}\right) \quad (2)$$

The photon dispersion function w(q) for an optical branch in crystalline silicon is given by:

$$w^2(q) = A + B\cos(\pi q/2) \quad (3)$$

Where A=1.714×$10^5$$cm^{-1}$ and B=1×$10^5$$cm^{-1}$. The values of w and Γ are taken as 521cm^{-1} and 3.5 cm^{-1} respectively, corresponding to the natural line width and the peak position of the first order Raman line in the crystalline silicon, (a) is the silicon lattice constant (0.543nm) and L is the quantum confinement dimension.

However, the corresponding changes in the Raman line-width and asymmetry with the same change in the confinement parameter (*L*) using Eq. (1) do not agree with our experimental data. In order to quantitatively account for our experimental results, we have assumed that the Raman spectrum observed is as uper position of the first-order Raman scattering contributions from phonons confined in columnar structures with a distribution in their confinement dimensions. Assuming that the confinement size distribution is represented by a Gaussian function, N(*L*)=exp-[(*L*-L_o)/σ)], the resultant Raman intensity is the convolution of Eq. (2) with the Gaussian function, and is given by:[10, 14]

$$I(w) \alpha \int_{L_1}^{L_2} N(L) I'(w, L) dL \quad (4)$$

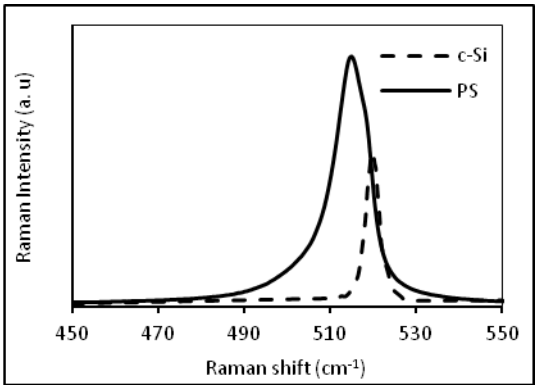

Fig. 1: Typical Raman spectra of silicon samples with a) stain etching at 20min b) c-Si sample.

In figure 2 the Raman spectra was plotted of PS samples. The experimental data are shown as dots, while the solid line is drawn to guide the Raman spectra by using the phonon confinement model by using equation 4. Figure 2(a) shows the Raman spectra of PS sample prepared with 20 min etching time and a 30W the power of US cavity. The spectra were recorded with different power (30 & 50) W. the Raman peak position shifts to a lower frequency 518cm^{-1} after etching. Furthermore, the Raman line is wide and asymmetric in comparison to the Raman line from crystalline silicon for which the line has narrow and symmetric shape centered at 521cm^{-1}. The line-shape asymmetry increases as the power of ultrasonic is increased from 30W to 50W, and the Raman peak position remains close to 518cm^{-1}. The observed changes in the Raman line shape as a function of the power of ultrasonic may be attributed to the spatially dependent size

distribution of nanocrystallites in our sample. The line-shape asymmetry ratio Γa/Γb increases from a value of 1.05 to 1.22 when the power of ultrasonic varies from 30W to 50W.

The smaller asymmetry ratio in the Raman line obtained with 30W implies large nanostructure size in to the sample compared to the layer obtained with 50W. The dependence of the asymmetric ratio on the power of US is plotted in table 1. smaller asymmetry ratio of the Raman line for 30W power of US implies larger nanocrysalline size were found deeper into the sample compared to those in the upper layer of the reconstructed surface.

The experimental data are fitted by phonon confinement model and the best fitting parameters are given in table (1). Slight variations of the Raman lone shape were noticed after PS layer formation. The corresponding FWHM was 9.5 cm^{-1} compared to that for the bulk of value 3.5 cm^{-1} and there was noticeable change in the Raman peak position for this layer. The mean value of nanocrysalline size estimated for this condition was 4 nm. The asymmetry ratio for PS was 1.06. When the ultrasonic treatment applied through the etching processes (30W), the Raman peak shifts to 516.6 cm^{-1}. The FWHM and asymmetry ratio increases to 9.51 cm^{-1} and 1.16 respectively, due to a reduction of the nanocrystallite mean size to 5 nm. The nanocrystallite size increases to 8.5nm, when the power of US cavity increases to 50W. The Raman peak shifts 520cm^{-1}. The FWHM and asymmetry ratio decreases to 3.7 cm^{-1} and 1.22 respectively.

Table 1: Comparison of Raman parameters for samples at different condition of preparation.

Sample	L (nm)	FWHM (cm^{-1})	Raman peak position (cm^{-1})	Γ_a/Γ_b
Crystalline silicon	-	3.5	521	1
Chemical etching only	5	6.87	516.6	1.06
Chemical etching +US(30W)	4	9.518	515	1.16
Chemical etching +US(50W)	8.5	3.7	520	1.22

It turns out from Eq. (4) that the peak positions ofthe Raman line are mainly determined by L_o, where N(L) is a maximum. In the case of 20 min etching, choosing L_o=50nm gives a peak position close to the observed value of 516.6 cm^{-1}. For our calculations, we chose a minimum value of L_1=57nm and the values of L_2 and σ to fit experimental data of Figure 2(a) was 4.2 nm and 4nm respectively. Best-fit values of L, L_1, $L_2$and σ for various the powers of ultrasonic values and the spectra calculated are shown by the solid line curves in Figure 2(a).

For the sample prepared at 20 min and 30W power of ultrasonic, L_2=*46nm*, σ=4nm and the asymmetry ratio of this sample that there is apreponderance of small nanoparticles with L_o<*4nm*. The full width at half-maximum is 6.87 cm^{-1} in this case. For sample prepared at 20min and 50W power of ultrasonic, the penetration depth (thickness) increases to 1250 nm, due to of escape of hydrogen bubbles and other etched chemical species from the porous silicon pillars' surface. The effect is attributable to effective change in the concentration of free holes carriers. Ultrasound has led to indicating probably a change in bonding configuration, and increase in oxidation. In this case, a good fit is obtained for L_o=*8.5nm*, while σ remainsun changed at 4nm, the FWHM being 3.7cm^{-1}. Large nanocrystals are observed at these power values. On the whole, the Raman data indicate the presence of nanocrystals of different sizes. The nanocrystallite size varies between 4nm to 8.5nm.

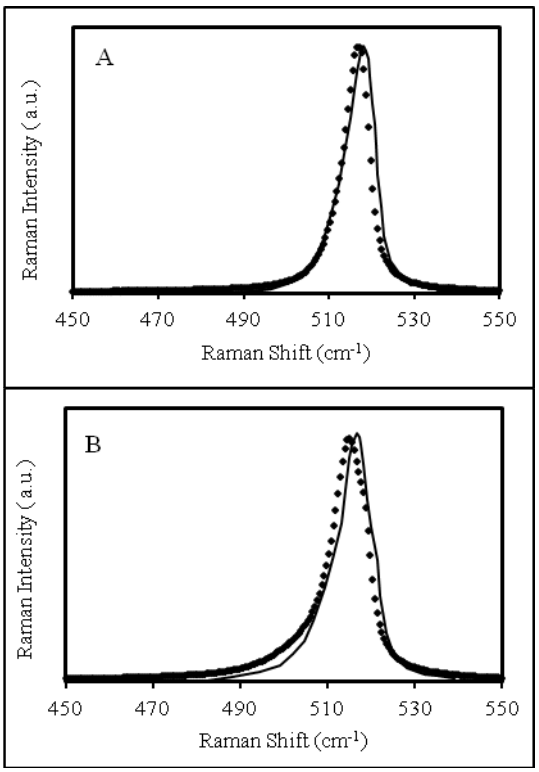

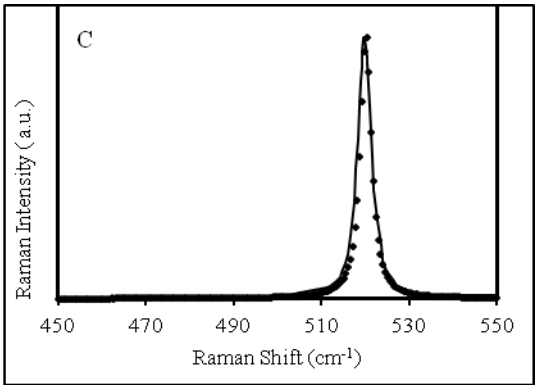

Fig. 2: Raman scattering spectra of PS layer on c-Si samples with a)chemical etching only b) chemical etching with 30W c) chemical etching with 50W. Measured (dots curve) and calculated Raman spectra using the phonon confinement model.

Figure 3 shown the dependence of nanocrysallite size on the power of ultrasonic cavity. when etching process starts at case one (without ultrasonic), a further reduction of the nanocrystallite size occurred with power of ultrasonic cavity 30W as an optimum value and these smallest nanocrystallites were distributed at the top of the PS layer and got progressively removed with increasing the power of ultrasoninc cavity to 30W. The removal of smaller nanocrystallites continues with increasing ultrasonic cavity power up to 50W and larger nanocrystallites are left behind. This explanation was supported by the observed increase in the PS layer thickness with increasing power of US cavity of more 50W [19].

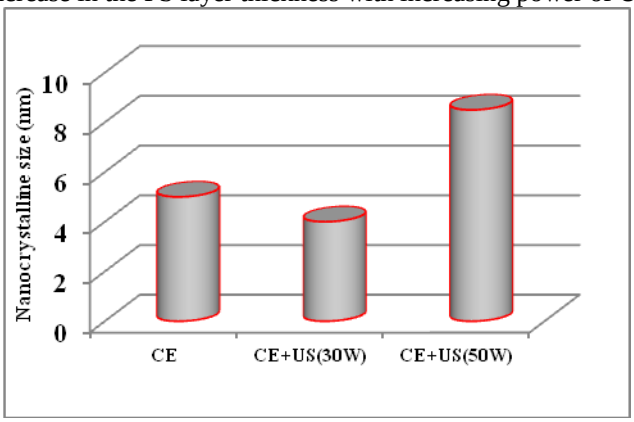

Fig. 3: Variation of the nanocrystalline size with power of ultrasonic for the chemical etching.

4. Conclusion

The porous layer of silicon was fabricated by means of the chemical etching in (HF and HNO_3) solution using different US excitation from 30 to 50 W. Ultrasonically enhanced etching process causes the reaction between the etchant and the silicon wafer to proceed more rapidly along the vertical in the silicon pores than laterally (coefficient of anisotropy (average depth of pores/average width of pores) increases from 7.31 to 158.4).

The corresponding changes in Raman spectra as a function of ultrasonic power.Comparing the Raman spectra from PS at different US power, with that of c-Si, one can see that Raman line of the PS is red-shifted and highly asymmetric till P= 50W. It is known that the asymmetric Raman line shape can arise due to the phonon confinement in the nanoscale crystallites. In PS these can be either approximated to cylindrical.

References

[1] Schirone L., Sotgiu G. and Califano F. P.,(1997), Thin solid films 297, pp. 296-198.
[2] Garcia J. L. , Palma R. M., Manso M. and Duart J. M., , (2007), Sensors and Actuators B 126, pp.82-85.
[3] Prabakaran R., Kesavamoorthy R. and Singh A., (2005), Bull. Mater. Sci. 28(3), pp.219-225 (2005).
[4] Rasheed R. G., Alhamdani A. H. and Dawood Y. Z.,(2010), Journal material science and engineering 4(3).
[5] BrunettoN. and Amato G., (1997) Thin Solid Films 297, pp.122124.
[6] Al-Dwayyan A. S. , Khan M. N., and Al-Salhi M. S., (2012), Journal of Nanomaterials 713(203), pp. 1-7.
[7] Wu M. H., Mu R., Ueda A., Henderson D. O. and Vlahovic B., (2005),Materials Science and Engineering B 116(3), pp. 273-277.
[8] Zh. Sui, P. P. Leong, I. P. Herman, G. S. Higashi and H. Temkin, (1992).Appl. Phys. Lett. 60(17), pp. 2086 .
[9] Mavi H. S, Rasheed ., B. G., Soni R. K., Abbi S. C. and Jain K. P., (2001), Thin Solid Films 397, pp.125-132.
[10] Liu L. Z.,. Wu X. L, Zhang Z. Y., Li T. H., and Chu P. K., (2009) Appl. Phy. Lett. 95, pp.93-109.
[11] L Q.i, W. H. Tan, Guo J., Kang Y., (2010), Optics and Lasers in Engineering 48,pp. 1119-1125.
[12] Yang M. , Huang D. , Hao P., Zhang F., Hou X., and Wang X., (J. Appl. Phys. 75, pp. l-5.
[13] Gouadec G. and Colomban Ph, (2007) Progress in Crystal Growth and Characterization of Materials 33, 56.
[14] Lemusa R. G.,. Rodriguez C. H., Hander F. B. and Martıınez J. M., (2001), Solar energy materials & solar cells 72,pp. 495-501.
[15] Pawlak B. J., Gregorkiewicz T., and Ammerlaan C. A., (2002), Phys. Rev. B 64(115308), pp. 1-9.
[16] Kalem S., Yavuzcetin O. and Altineller C., (2000), Journal of Porous Materials 7, pp.381-383.
[17] Liua Y., Xiong Z. H., Liu Y., Xu S. H., Liu X. B., Ding X. M. and Houa X. Y., (2003), Solid State Communications 127,pp. 583-588.
[18] Troia A., Giovannozzi A. and Amato G., (2009) Ultrasonics Sonochemistry, 16, pp. 448-451.

[19] Dawood Y. Z., Al-Hamdani A. H. and Zayer M. Q., (2013) ARPN Journal of Engineering and Applied Sciences, 8(2), pp.105109.
[20] Kuzik L. A., Yakovlev V. A. and Mattei G., (1999), Appl. Phy. Lett. 75(13), pp. 27-32.